Research Article

Feng Qiu, Junxia Qiu*, Heng Feng, Huajie Wang, Hongliang Qian, Xiaofei Jin, Kaiyuan Wang, and Feng Fan

Calculation method of stability bearing capacity of transmission tower angle steel considering semi-rigid constraint

https://doi.org/10.1515/cls-2022-0017
Received Sep 07, 2021; accepted Feb 11, 2022

Abstract: The angle steel member is the most commonly used component form of the transmission tower structure. Considering its connection characteristics, we must deal with its stability analysis under semi-rigid constraint conditions for the proper study of the overall structure's mechanical performance. Therefore, in order to establish a simple and high-precision method suitable for the ultimate bearing capacity analysis of the transmission tower, we build the refined finite element models of typical steel tower joints, analyze its moment-rotation curve and utilize simulation technique of spring elements to acquire the calculation method of its single angle stability bearing capacity, which is considering initial imperfection and residual stress. Furthermore, we analyze its bearing capacity under different constraint conditions such as rigid, semi-rigid and articulated connection. The results show that it is necessary to consider joint stiffness in the bearing capacity analyses. Finally, it's confirmed that the calculation results of this method agree well with the experimental data, which validates its high accuracy. Therefore, the method provides technical support for high efficient component stability simulation in overall stability analyses of the transmission steel tower.

Keywords: single angle; stability bearing capacity; moment-rotation curve; semi-rigid joint; transmission tower

1 Introduction

As the lifeline engineering, the transmission tower is an important part of the power line system so its secure research has important significance. However, its complicated load state is very likely to cause structural damage and lead to the interruption of the power transmission, which will not only directly cause high economic losses, but also badly affect people's normal life. The production activities are shown in Figure 1. Related engineering accidents [1–3] show that the failure mode of the transmission tower is generally caused by the instability of the angle steel members. Therefore, it is significant to study the ultimate bearing capacity of high-voltage transmission towers and improve the calculation accuracy of its ultimate bearing capacity from the angle of steel members to guarantee the normal operation of the power system.

At present, the calculation of the ultimate bearing capacity of the angle steel transmission tower mainly takes the joint as an ideal hinge or rigid connection [4–7]. Kennedy and Madugula [8] carried out an experimental study on 72 single-angle presser bars with rigid joint and articulated joint connections at the ends, in order to provide verification of the theoretical solutions for flexural, torsional-flexural, and plate buckling. Baton [9] and Liu [10] studied the compression test of a lot of equal-edge and non-equal-edge angle steel and the end connection was articulated by spherical hinge bearings, by which the ultimate compressive load capacity of single steel angles subjected to eccentrically applied axial load was investigated. Cao *et al.* [11] restrained the rotation of angle around

***Corresponding Author: Junxia Qiu:** Department of Civil Engineering, Harbin Institute of Technology at Weihai, Weihai 264209, China; Email: Junxia_Qiu@163.com
Feng Qiu, Feng Fan: School of Civil Engineering, Harbin Institute of Technology, Harbin 150090, China
Heng Feng: Central Southern China Electric Power Design Institute Co., Ltd. Of China Power Engineering Consulting Group, Wuhan 430061, China
Huajie Wang, Hongliang Qian: School of Civil Engineering, Harbin Institute of Technology, Harbin 150090, China; Department of Civil Engineering, Harbin Institute of Technology at Weihai, Weihai 264209, China
Xiaofei Jin: China Construction First Group Corporation Limited, Beijing 100161, China
Kaiyuan Wang: Department of Civil Engineering, Harbin Institute of Technology at Weihai, Weihai 264209, China

Open Access. © 2022 F. Qiu *et al.*, published by De Gruyter. CC BY This work is licensed under the Creative Commons Attribution 4.0 License

Figure 1: Collapse accidents of transmission tower

Figure 2: Actual angle joint of transmission tower

the normal axis of the connecting leg rigidly when they calculated the bearing capacity.

Actually, as shown in Figure 2, the angle steel transmission tower usually adopts bolts and joint plates to connect the angle steel with the main bar on one leg so that this connection joint become semi-rigid between the hinge and rigid connection which can withstand a certain bending moment and get a certain rotational capacity. In Usami's single angle experiment [12], the ultimate bearing capacity of the angles with rigid constraint is higher 40% to 100% than that of hinged constraint. Roy [13] studied the second-order effect caused by the large displacement of the transmission tower structure, and the results showed that the second-order stress caused by joint stiffness cannot be ignored for UHV transmission tower. Therefore, regarding the node as an ideal hinge or rigid joint simply does not conform to the actual situation and affects the calculation accuracy of the ultimate bearing capacity of the structure.

In the actual project, the constraint action of the end of angle steel also has the characteristics of semi-rigid. To simulate the influence of the joint's actual stiffness accurately and restore the real constraint conditions of the end of angle steel, KeKe [14] and Kettler *et al.* [15] built the entity-unit models of bolts and gusset plate at the end of angles, which investigated the shear lag effect on the behavior and ultimate tensile capacity of high strength steel (HSS) tension angles with bolted and welded connections [14], and focused on the presentation of the influence of realistic end support conditions at the gusset plates on the member capacity in compression [15]. But in this method, each entity-unit model of angle with different slenderness ratio should be built, which leads to huge calculation expense, and the method using entity-unit model can't be used in whole tower structure analyses. So, it's necessary to establish a simple and high-precision method of angle capacity calculation, which is also suitable for ultimate bearing capacity analyses of transmission tower.

In this paper, the moment-rotation curve of the angle joint is gained by building a refined finite element model of a typical steel tower joint. And the practical calculation method for establishing curves is proposed with the Kish-Chen power model [15] which expressed the general quantitative relationship between bending moment and rotation of semi-rigid connections. The accuracy of the method is verified by the numerical simulation. Then based on the moment-rotation curve obtained by the calculation method, spring elements are applied to both ends of angle members to simulate the semi-rigid constraint form joints, the extreme point of the load-displacement curve is taken as the stable bearing capacity. In this way, the calculation method of the single angle stability bearing capacity is presented and its accuracy is verified by related experimental data, which provides technical support for the refined simulation calculation of the overall ultimate bearing capacity of the transmission tower structure.

2 Calculation method for moment-rotation curve of joint

The overall instability mode of a single angle is complex. The principal axes of the angle steel section (z axis and w axis in Figure 3) are not parallel with the connected leg, by which the load is transferred. Temple and Sakla examine the load-carrying capacity and behavior of a single-angle compression member welded [16]. The angle steel is under biaxial bending and compression, and the bucking axis is the u axis which is located between x axis and y axis. Thus, the constraint forms of rotation around x axis and y axis of angle both have some influences on bearing capacity. In practical structures, the direction around x axis is outside the plane of the gusset plate, of which the flexural rigidity in this direction is weak, so the rotation in this direction can be treated as free. The end constraint of angles around y axis is mainly researched in this paper, and the hinged connection and rigid connection are both relative to this direction.

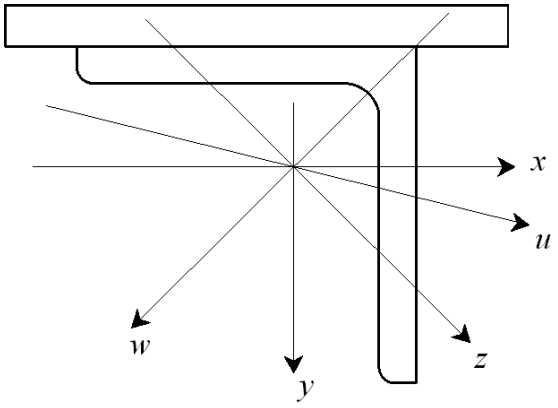

Figure 3: Instability axes of single angle

2.1 The finite element model of angle joint

As shown in Figure 4, a typical angle joint of 800v high voltage transmission tower is selected as an example model. The section of secondary angle is 45 × 5mm, and that of main angle is 75 × 6mm. The thickness of gusset plate is 6mm. Secondary angles are connected to the main angle by two M16 bolts.

The refined finite element model of angle joint is built by ANSYS. Angles, gusset plates and bolts are established by SOLID 185, which is often used to construct the three-dimensional solid structure. CONTA174 and TARGE 170 are

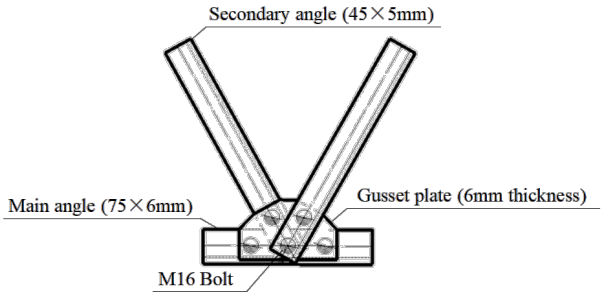

Figure 4: Typical angle joint of transmission tower

used to simulate the contact surface and target surface when the components contact. The material of the secondary angle is Q235 and its Poisson's ratio is 0.3. The main angle and the gusset plate are made of Q420 steel. Bolts in the model are 9.9 high-strength bolts. The bilinear kinematic constitutive model is adopted for all materials, the elastic modulus is 206000 Mpa, and the tangent modulus of the hardening section is 2% of the elastic modulus, which is 412 Mpa. The main angle is restrained on two ends. Uniform surface load q is applied to the top end of the left secondary angle so that the rotational stiffness of the joint could be studied. The bending moment of joint (M_y) is shown as Eq. (1) and Figure 5.

$$M_y = qA \times L \tag{1}$$

Where A is the sectional area of secondary angle, L is the distance between top end of the angle and center of lower bolt.

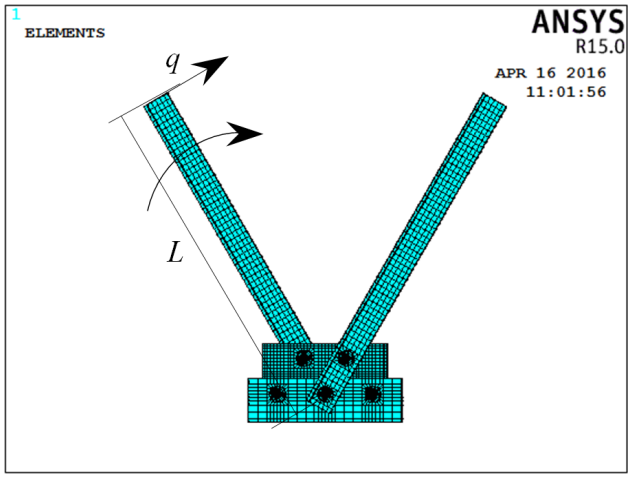

Figure 5: Finite element model of angle joint

2.2 Analysis of the semi-rigid performance of angle joint

The deformation graph of the joint model is shown in Figure 6. The secondary angle is bent by the loads. The maximum displacement occurred at the end of the angle, and it reached 4.3cm. From Figure 7, It is seen that the part of the angle is constrained by bolts rotated, which indicates the semi-rigid constraint of secondary angle from the angle joint. The von Mises stress contour of the left secondary angle is shown in Figure 8. Almost all the sections where bolt holes were located had been plastic areas, which lead to the disruption of the model.

As shown in Figure 9, line AB is selected as the reference line to calculate the rotation of the secondary angle. Point A′ and B′ are displaced to joint positions of point A and B. Line AB is translated to be line CB′, and then CA′ is the relative displacement from point A to B. Then the rotation angle θ can be calculated with Eq. (2).

$$\theta = \angle \mathrm{CB'A'} \approx \frac{\mathrm{A'C}}{\mathrm{A'B'}} = \frac{\sqrt{(z_B - z_A)^2 + (x_B - x_A)^2}}{L_{AB}} \quad (2)$$

Where L_{AB} is the distance from point A to B, z_A and z_B are the z-direction displacement of A and B, x_A and x_B are the x-directional displacement of A and B.

The moment-rotation curve of the angle joint shown in Figure 10 is established based on θ and M_y. The slope of the curve at the origin is the initial rotation stiffness of the joint (K), which is calculated to be 259.17 kN·m/rad. And the ultimate moment (M_u) is 1.32 kN·m.

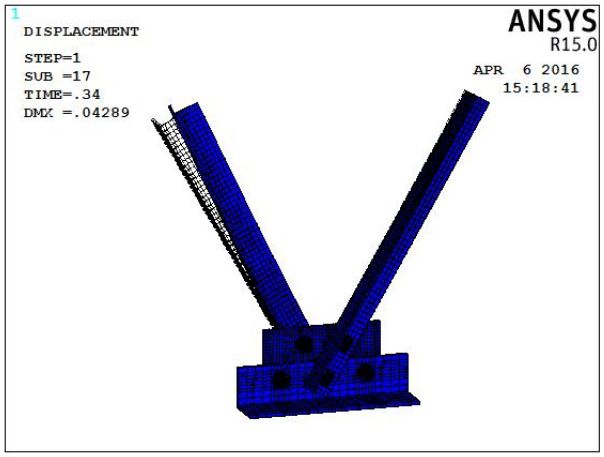

Figure 6: Overall deformed shape of joint model

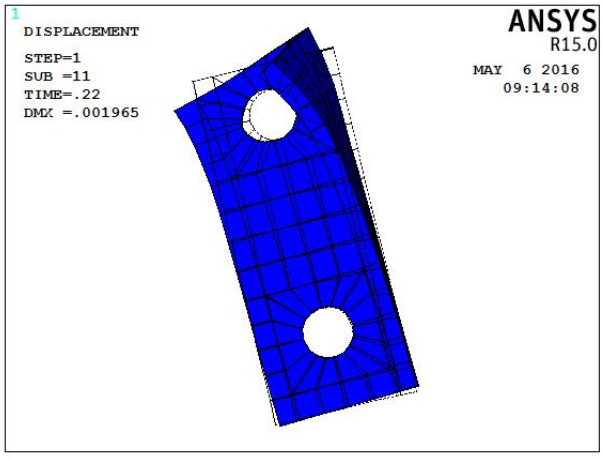

Figure 7: Local deformation of secondary angle (Magnified 10 times)

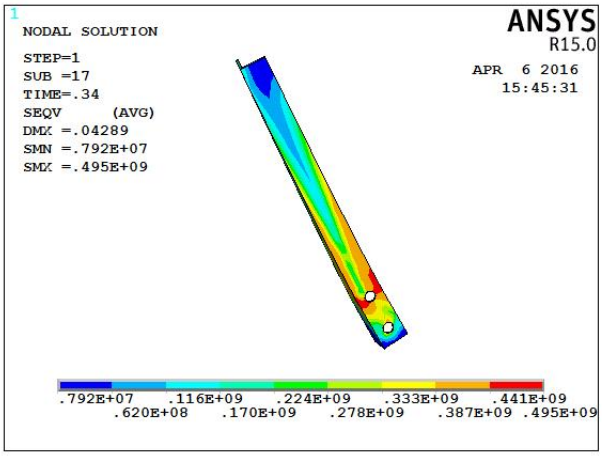

Figure 8: Equivalent stress nephogram of left secondary angle

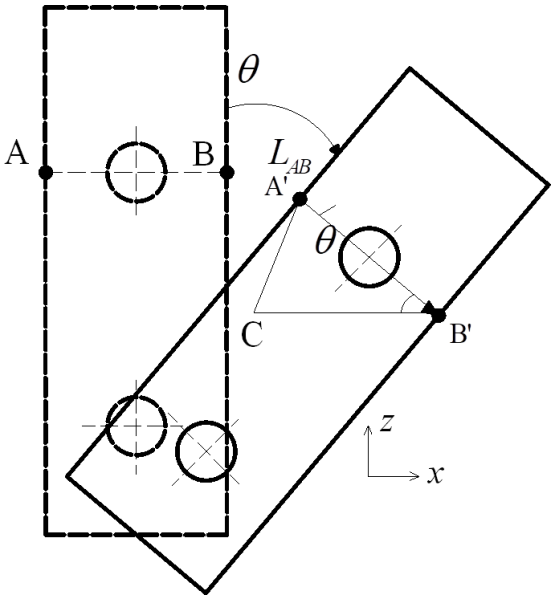

Figure 9: Rotation schematic diagram of angle

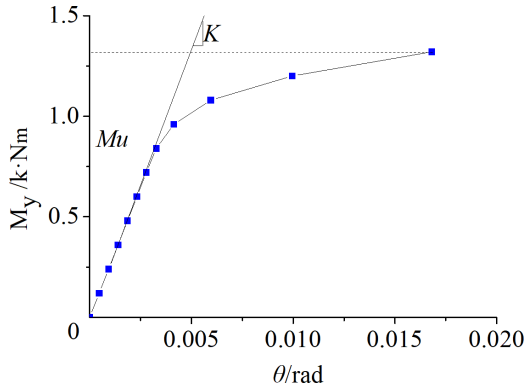

Figure 10: Moment-rotation curve of angle joint

2.3 The influences of axial force and end constraint on moment-rotation curve

The bending moment is applied to the second angle when the semi rigidity is analyzed, and the top end of the right angle is completely free. In actual structures, the angle members mainly suffer from the axial force, and the right angle is restrained by the joint. In order to prove the correctness of the moment-rotation curve, the influences of the axial force and constraint in the right angle on moment-rotation curve are studied.

Four contrasting joint models are built based on the example model. Axial forces sized 20kN, 40kN and 60kN are applied to secondary angles of models 1-3. The right secondary angle of model 4 is restrained, and it can just deform axially. The calculation results of the initial rotation stiffness and the ultimate moment of contrasting models are shown in Table 1. With the increasing axial force of the second angle, the initial rotational stiffness decreases slightly. And the maximum decreasing amplitude is just 2.3%. The increased amplitude from the constraint of the right secondary angle is less than 1%. All of the five models' ultimate moments are 1.32 kN·m. Based on the analysis above, it's seen that the influences of the axial force and constraint in the right angle can be ignored when the moment-rotation curve is established.

2.4 Simplified calculation method for establishing moment-rotation curve

Since it's complicated to gain the moment-rotation curve by building refined finite element model of the angle joint, the simplified calculation method of establishing the curve is of good value. Based on Kishi-Chen's research, the Kishi-Chen power function model [17] is selected as the basic model to become the simplified calculation, and calculation equations of the model are shown in Eq. (3) and Eq. (4).

$$M = \frac{K_i \theta}{\left[1 + \left(\frac{\theta}{\theta_0}\right)^n\right]^{1/n}} \tag{3}$$

$$\theta_0 = \frac{M_u}{K_i} \tag{4}$$

Where K_i is the initial rotation stiffness of the joint, M_u is the ultimate moment, and n is the shape parameter of the moment-rotation curve.

With the Kish-Chen power model, the moment-rotation curve of angle joint can be established by K_i, M_u and n, so it's necessary to determine the relationships between these three parameters and the joint model parameters. The width and thickness of the secondary angle (b_1 and t_1), the thickness of gusset plate (t), the width and thickness of the main angle (b_2 and t_2), the steel strength of angle (f_y), the diameter, distance and number of bolts (d, s and p) are chosen to be the model parameters, some of which are shown in Figure 11. In total 135 finite element models of angle joint are built and calculate K_i, M_u of each model. The values of n of element models are fitted according to the moment-rotation curves with the least square methods. Parts of the results are shown in Table 2.

Zhao analyzed the influences of model parameters on K_i, M_u and n, the parameters which have significant influences are selected to fit the formulas [18]. The form of fit formula is shown as Eq. (5).

$$x = e^{k1} {b_1}^{k2} {t_1}^{k3} d^{k4} t^{k5} {b_2}^{k6} {t_2}^{k7} {f_y}^{k8} s^{k9} p^{k10} \tag{5}$$

Table 1: Calculation results of comparison models

Models	Axial force/kN	If the right angle is restrained	Initial rotational stiffness	Ultimate moment
Example model	0	No	259.17	1.32
Contrast model 2	20	No	257.77	1.32
Contrast model 3	40	No	255.83	1.32
Contrast model 4	60	No	253.28	1.32
Contrast model 5	0	Yes	261.00	1.32

Table 2: Parameters and calculation results of angle joint models

Number	b_1/ mm	t_1/ mm	t/ mm	p	d/ mm	s/ mm	b_2/ mm	t_2/ mm	f_y/ MPa	K_i/ kN·m/rad	M_u/ kN·m	n
1	50	4	6	2	16	70	75	6	235	267.18	1.20	4.615
2	50	5	6	2	16	70	75	6	235	305.49	1.56	3.700
3	50	6	6	2	16	70	75	6	235	337.52	1.92	3.194
4	63	4	6	2	20	70	75	6	235	373.56	1.80	3.829
5	63	5	6	2	20	70	75	6	235	423.13	2.40	3.071
…	…	…	…	…	…	…	…	…	…	…	…	…
131	90	8	8	3	16	70	140	12	235	1270.85	6.30	4.081
132	90	8	8	3	24	70	140	12	235	1468.99	9.24	3.996
133	100	10	8	3	16	70	140	12	235	1554.77	10.56	3.583
134	100	10	8	3	24	70	140	12	235	1841.20	4.80	4.518
135	90	12	8	3	20	70	140	12	235	1646.80	10.80	4.175

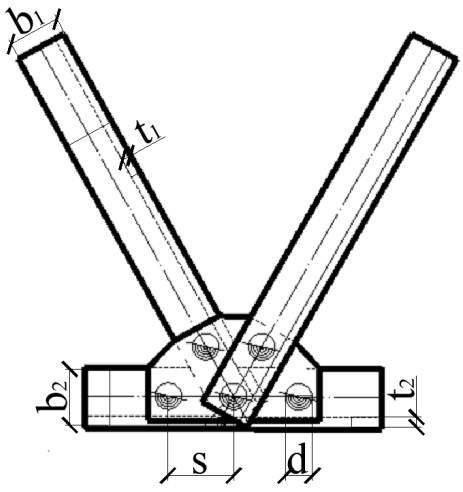

Figure 11: Some of the model parameters

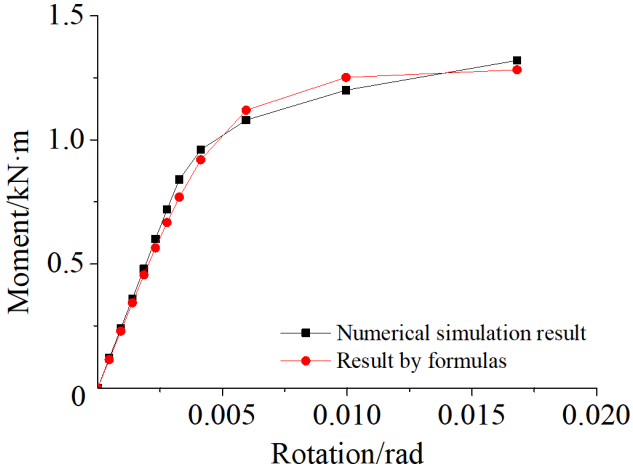

Figure 12: Comparison between formula calculation moment rotation curve and numerical simulation result

where x is the parameter which need to be fitted, e is the natural constant.

The fitting results of K_i, M_u and n are shown as Eqs. (6)–(8).

$$K = e^{-4.702540} b_1^{1.362327} t_1^{0.436146} d^{0.391488} t^{0.233223} \cdot b_2^{0.348980} t_2^{-0.095594} s^{0.251754} n^{0.603790} \quad (6)$$

$$M = e^{-14.199584} b_1^{1.709699} t_1^{0.786713} f_y^{0.788590} \cdot s^{0.417859} n^{0.870692} \quad (7)$$

$$n = e^{-0.846650} b_1^{0.150867} t_1^{-0.674903} d^{-0.162979} t^{0.134414} \cdot b_2^{-0.118727} t_2^{0.419483} f_y^{0.324126} s^{0.067652} p^{0.743568} \quad (8)$$

Since the example model is not included in the 135 models, it can be used to verify the accuracy of these formulas. K and M_u of the example model is calculated by Eq. (6) and Eq. (7). The value of K is 247.81 kN·m/rad, and the error between the formula result and the numerical simulation result is 4.4%. M_u is calculated to be 1.30, and the error is 1.5%. The value of n is calculated by Eq. (8). The moment-rotation curve of the example model is established with the results of formulas, and it is compared with the numerical simulation result, which is shown in Figure 12. It is seen that the curve by formula results agrees well with the numerical one. The average error of the data is 5.04%, and the accuracy of these equations is high. So the moment-rotation curve can be established directly by Eq. (3) to Eq. (8) with model parameters, which is much easier than the way of a building refined finite element model.

3 Calculation method of single angle bearing capacity

In order to improve computational efficiency, the single model is built by SHELL 181 (a kind of element which only needs to input thickness and does not need to generate solid for thin-walled structure) instead of SOLID 185. And COMBIN 39 (a one-way element with nonlinear function, which can input generalized force deformation curve) is applied to both ends of the angle steel model according to the moment-rotation curve, which is used to simulate the semi-rigid constraint.

The simplified model of single is shown in Figure 13. The restraint rotation around y axis is applied to nodes on the lines AB and DE, and the rotational stiffness of springs is defined with the moment-rotation curve of the joint. The displacement in y direction of the nodes in the middle of lines AB and DE is restrained, and the displacement in x direction of points B and E is restrained. The displacement constraint in z direction is applied to the nodes in the middle section of the angle steel.

The influence of initial imperfection and residual stress is considered when the bearing capacity is calculated. The first mode of eigenvalue analysis is selected as the shape of initial disfigurement, and the maximum lateral displacement of a single is changed to be 1/1000 of the single length by adjusting node coordinates. Zhou *et al.* established a distribution model of residual stress which is shown in Figure 14 [19]. And the uniform load p is applied to the nodes on line AB and DE.

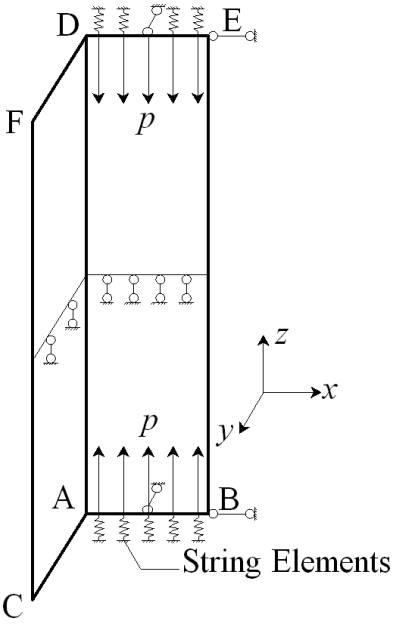

Figure 13: Simplified calculation model of angle

The section of example Q235 single angle model is 45 × 5mm (the material properties of the finite element model are shown in Section 2.1), and the slender ratio of the weak axis (λ_z) is 170. The contour graph of Von Mises stress when the single is damaged is shown in Figure 15. And the load-y directional displacement curve of the central node of the angle is shown in Figure 16. The extreme point of the curve is taken as the stable bearing capacity. When the load exceeds this point, the following curve will show a downward trend. This shows that the load corresponding to the extreme point is the maximum load that the component can withstand. If the component wants to maintain balance, it needs to reduce the end load, otherwise, the component will be in the unstable equilibrium state. It is seen that the single bucked overall when the load came up to 31.83kN. The maximum displacement in the y direction of the node is 16mm, and the maximum stress reached 300 MPa.

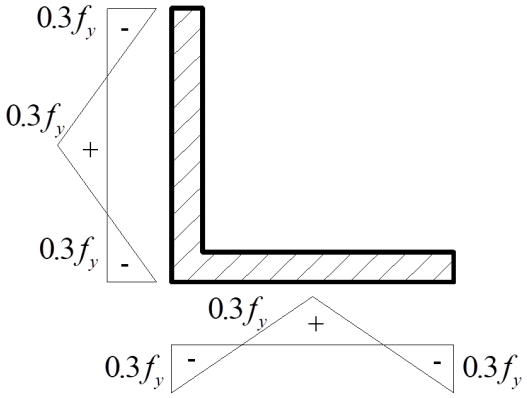

Figure 14: Distribute form of residual stress

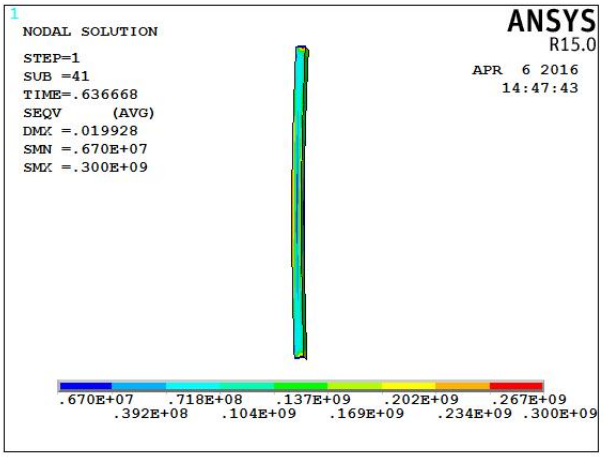

Figure 15: Equivalent stress nephogram of angle model

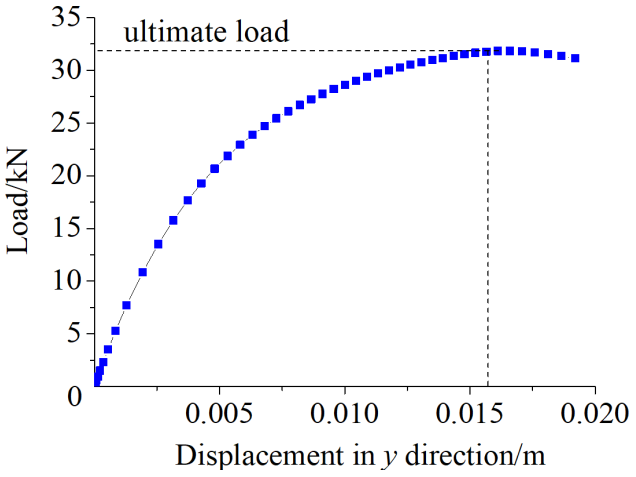

Figure 16: Load-y directional displacement curve

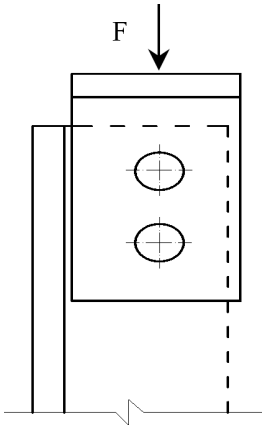

Figure 17: End constraint condition of test component

4 Accuracy verification of the method

Zhou *et al.* summed up the restraint conditions of the double-bolt connection end from a series of experiments about single angles by the Beijing Electric Power Research Institute [19]. The end of test angles was connected with the gusset plate by two M16 bolts, which is similar to the example single in this paper. And the end constraint in the test is shown in Figure 17. The capacities of the test angles are calculated with the method which is proposed in this paper, and the results are shown in Table 3. It's seen that the calculation results agree well with test data. The maximum error is 10.3%, and the average one is 6.4%. Therefore, this method has high precision.

5 Influence of joint stiffness on bearing capacity

In order to study the influence of the joint stiffness on the bearing capacity, the bearing capacities of a single angle under different constraint conditions such as rigid connection, connection and hinged connection are calculated. The example model is the angle with a semi-rigid connection whose schematic diagram of shown in Figure 13. The schematic diagram of a single angle model with a. rigid connection is shown in Figure 18(a). All the freedom degrees except rotation around x axis of nodes on line AB are restrained. And the nodes on the line DE can just move in z direction. The uniform load is applied on line DE. The schematic diagram of a single angle model with a hinged connection is shown in Figure 18(b). The constraint conditions of the model are similar to that of the example model, except that there are no string elements at the ends of the angle.

Table 3: Comparison between calculation results of presented method and experimental data

Number	Section	Slenderness ratio λ_z	Yield strength f_y/MPa	Test results N_1/kN	Calculation results with method proposed in this paper N_2/kN	Error $\frac{N_2-N_1}{N_1} \times 100\%$
1	∠45 × 5	203	280	27.3	26.4	3.2%
2	∠45 × 5	170	280	32.9	31.8	3.4%
3	∠56 × 5	136	280	59.5	53.4	10.3%
4	∠63 × 5	120	280	66.2	70.3	6.2%
5	∠45 × 5	101	280	56.4	53.0	6.0%
6	∠56 × 5	90	280	77.6	73.9	4.5%
7	∠45 × 5	84	280	66.0	59.6	9.7%
8	∠56 × 5	67	280	79.3	73.2	7.7%

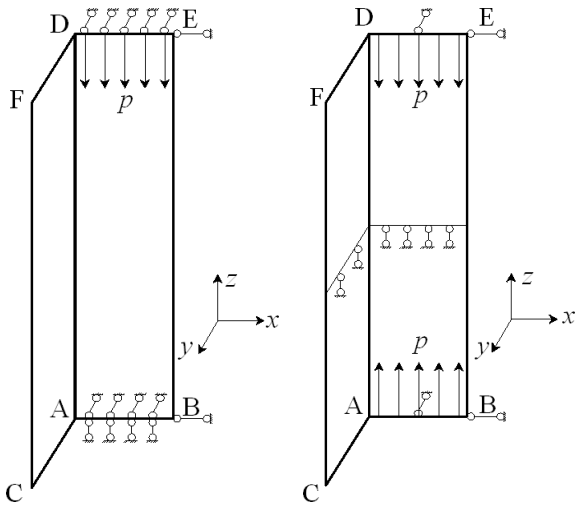

(a) Rigid connection **(b)** Articulated connection

Figure 18: Connection schematic diagrams

The bearing capacities of the singles whose sections are 45 × 5mm under three constraint conditions are calculated, and the results are shown in Figure 19. The capacity of angle with semi-rigid constraint is between that of rigid angle and hinged angle. The capacity of rigid angle is 16.7% higher than that of semi-rigid constraint angle on average. And the capacity of the semi-rigid constraint angle is 14.7% higher than that of the hinged one. So, it is necessary to take into account joint stiffness in single angle bearing capacity analysis.

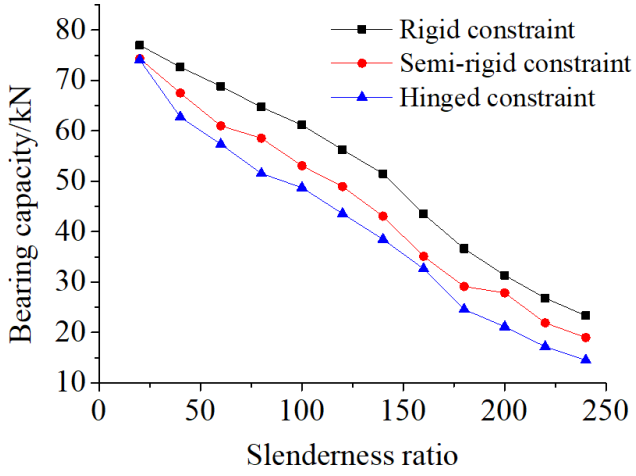

Figure 19: Angle stability capacities under different constraints

6 Conclusions

The calculation method of single angle bearing capacity is studied in this paper, and the conclusions are as follows:

The refined finite element model of angle joint is built, and the semi rigidity of the joint is analyzed. The practical formulas of establishing the moment-rotation curve of the angle joint are fitted. The curve can be gained with these equations instead of building a finite element model, which can improve computational efficiency.

According to the moment-rotation curve, the calculation method of single angle stability bearing capacity considering initial imperfection and residual stress is presented by utilizing the simulation technique of spring elements. And the accuracy of this method is verified with the related test data.

Based on the calculation results of the single angles with different constraint conditions, it is seen that the capacity of rigid angles is 16.7% higher than that of semi-rigid constraint angles on average. And the capacity of the semi-rigid constraint angles is 14.7% higher than the hinged one. So, it is necessary to take into account joint stiffness in single angle bearing capacity analysis.

Acknowledgement: This research was funded by the General Program of the Natural Science Foundation of Shandong Province (ZR2019MEE047), the National key research and development project of China (No. 2020YFB1901403), CSCEC Technical and Development plan (CSCEC-2020-Z-35).

Author contributions: All authors have accepted responsibility for the entire content of this manuscript and approved its submission.

Conflict of interest: The authors state no conflict of interest.

References

[1] McCarthy P, Melsness M. Severe weather elements associated with September 5, 1996 hydro tower failures near Grosse Isle. Manitoba, Canada: Manitoba Environmental Service Centre, Environment Canada; 1996. p. 21.

[2] Qiang X, Zhang J. Experimental study on failure modes and retrofitting method of latticed transmission tower. Eng Struct. 2021;226:111365.

[3] Dempsey D, White HB. Winds wreak havoc on lines. Transmission and Distribution World. 1996;48(6):32–7.

[4] Albermani F, Kitipornchai S. Numerical simulation of structural behaviour of transmission towers. Thin-walled Struct.

2003;41(2):167–77.
[5] Albermani F, Mahendran M, Kitipornchai S. Upgrading of transmission towers using a diaphragm bracing system. Eng Struct. 2004;26(6):735–44.
[6] Kitipornchai S, Albermani F, Kang WJ, Lam HF. Some practical aspects of modeling lattice towers. Proceedings of the Fourth International Conference on Advances in Steel Structures. 25 Jun 13-15; Shanghai, China. 2005;1:369-375.
[7] Albermani F, Kitipornchai S, Chan RW. Failure analysis of transmission towers. Eng Fail Anal. 2009;16(6):1922–8.
[8] Kennedy JB, Madugula MK. Buckling of Steel Angle and Tee Struts. J Struct Div. 1972;98(11):2507–22.
[9] Bathon L, Mueller WH 3rd, Kempner L Jr. Ultimate Load Capacity of Single Steel Angles. J Struct Eng. 1993;119(1):279–300.
[10] Liu Y, Chantel S. Experimental study of steel single unequal-leg angles under eccentric compression. J Construct Steel Res. 2011;67(6):919–28.
[11] Cao K, Guo YJ, Zeng DW. Buckling behavior of large-section and 420 MPa high-strength angle steel columns. J Construct Steel Res. 2015;111:11–20.
[12] Usami T, Galambos TV. On the Strength of Restrained Single Angle Columns Under Biaxial Bending. Papers and Reports of Japanese Society of Civil Engineering. 1971;191(191):31–44.
[13] Roy S, Fang SJ, Rossow EC. Secondary stresses on transmission tower structures. J Energy Eng. 1984;110(2):157–72.
[14] Ke K, Xiong YH, Yam MC, Lam AC, Chung KF. Shear lag effect on ultimate tensile capacity of high strength steel angles. J Construct Steel Res. 2018;145:300–14.
[15] Kettler M, Taras A, Unterweger H. Member capacity of bolted steel angles in compression–Influence of realistic end supports. J Construct Steel Res. 2017;130:22–35.
[16] Temple MC, Sakla SS. Single-angle compression members welded by one leg to a gusset plate. I. Experimental study. Can J Civ Eng. 1997;25(3):569–84.
[17] Kishi N, Chen WF. Moment-rotation semi-rigid connections, Structural Engineering Report No. CE-STR-87-29. School of Civil Engineering, Purdue University, West Lafayette, Indiana, USA. 1987.
[18] Zhao N. Study on load-bearing performances of semi-rigid joints and structure nonlinear analysis of UHV transmission tower [dissertation]. Chongqing: Chongqing University; 2014.
[19] Zhou R, Guo XN, Luo YF, Shen ZY. The research on bearing capacity of single angle struts with one-sided connection. In: Liu XL, editor.Proceeding of the Thirteenth National Symposium on Modern Structural Engineering. Tianjin, China.2013:864-870.